IOP PUBLISHING JOURNAL OF PHYSICS: CONDENSED MATTER

J. Phys.: Condens. Matter **19** (2007) 376110 (16pp) doi:10.1088/0953-8984/19/37/376110

Wet adhesion with application to tree frog adhesive toe pads and tires

B N J Persson

IFF, FZ-Jülich, 52425 Jülich, Germany

Received 12 April 2007, in final form 22 April 2007
Published 22 August 2007
Online at stacks.iop.org/JPhysCM/19/376110

Abstract

Strong adhesion between solids with rough surfaces is only possible if at least one of the solids is elastically very soft. Some lizards and spiders are able to adhere (dry adhesion) and move on very rough vertical surfaces due to very compliant surface layers on their attachment pads. Flies, bugs, grasshoppers and tree frogs have less compliant pad surface layers, and in these cases adhesion to rough surfaces is only possible because the animals inject a wetting liquid into the pad–substrate contact area, which generates a relative long-range attractive interaction due to the formation of capillary bridges. In this presentation I will discuss some aspects of wet adhesion for tree frogs and give some comments related to tire applications.

(Some figures in this article are in colour only in the electronic version)

1. Introduction

Surface roughness is the main reason for why macroscopic solids usually do not adhere to each other with any measurable strength, and even a root-mean-square roughness amplitude of ~ 1 μm is enough to completely remove the adhesion between normal rubber (with an elastic modulus $E \approx 1$ MPa) and a hard nominally flat substrate [1–3]. Biological adhesion systems used by insects and some geckos for locomotion are built from a relatively stiff material (keratin or chitin–protein composite with $E \approx 1$ GPa). Nevertheless, strong adhesion is possible even to very rough substrate surfaces by using *non-compact* solid structures consisting of either (a) *fiber-plate array* structures or (b) *foam*-like structures [4]. In order to optimize the binding to rough surfaces while simultaneously avoiding elastic instabilities, e.g. lateral bundling of fibers, many biological systems (e.g. spiders and geckos) use a hierarchical building principle, where the thickness of the fibers and plates (or walls) decreases as one approaches the outer surface of the attachment pad [5–7]. For spiders and some lizards the thickness of the fibers and plates at the surface of the attachment pads is so small that strong (dry) adhesion is possible even to very rough substrates [8]. However, for most insects (flies, bugs, grasshoppers) and for tree frogs, the thickness of the fibers and plates (or walls) is so large that negligible adhesion probably would

Figure 1. Tree frog toe pad. The diameter of the toe pad is of order ∼1 mm. Note the hexagonal array of cells or blocks, separated by grooves or channels. The diameter of one hexagonal block is of order ∼10 μm. Adapted from [15].

occur to most natural surfaces if both the pad surface and the substrate surface were dry [9][1], [10, 11]. For this reason flies, bugs, grasshoppers and tree frogs inject a wetting liquid into the pad–substrate contact area, which generates a relatively long-range attractive interaction due to the formation of capillary bridges. The liquid injected by insects seams to be a two-component emulsion comprising a lipid-like fraction and water-soluble nano-droplets [12, 13]; this liquid has been optimized by natural selection to wet most surfaces to which the insect has to adhere. In this presentation I will discuss some aspects of wet adhesion for tree frogs, but the results may also be relevant for other animals using smooth adhesive pads, e.g. grasshoppers [14].

2. Toe-pad contact mechanics and adhesion

2.1. Toe-pad construction

Figure 1 shows the toe pad of a tree frog [15]. Note that the pad surface is covered with an array of hexagonal (epithelial) cells (diameter $D_1 \sim 10$ μm) separated by *large* channels (grooves) (width $W_1 \approx 1$ μm, height (or depth) $H_1 \approx 10$ μm) that contain the fluid (watery mucus) which provides the toe pad's adhesive joint. Figure 2 shows a magnified view of a few of the hexagonal cells or blocks. The surface of each of these *large* blocks contains peg-like projections which we will refer to as the *small* blocks (diameter $D_2 \approx 0.2$ μm) surrounded by *small* channels (see figure 3) (width $W_2 \approx 40$ nm, height $H_2 \approx 0.2$ μm).

We will assume that the (mucus) fluid wets the surface of the toe pad. The free energy of the system is minimized when the liquid is localized to the channels, and if there is more fluid than can be contained in the channels it will also form a thin film on the (outer) surface of the

[1] In this reference it is shown that flies lose the ability to walk on inclined surfaces after walking for 15–30 min on a silica gel substrate. This can be understood if it is assumed that walking on the silica gel drains away all the adhesive liquid.

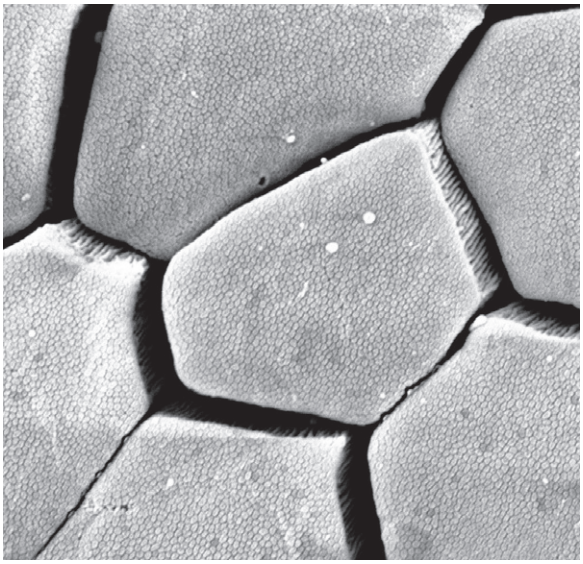

Figure 2. Magnified region of tree frog toe pad. The diameter of one hexagonal cell (or block) is of order $\sim$10 μm. Adapted from [15].

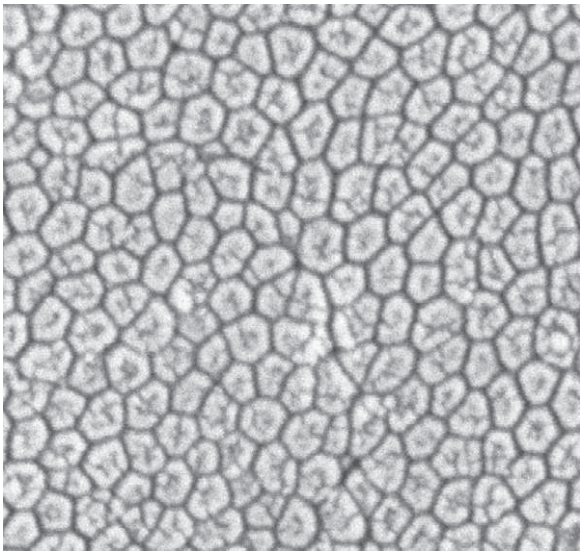

Figure 3. High magnification view of the surface of a single hexagonal cell showing peg-like projections. Adapted from [15].

toe pad. However, since the evaporation rate will be much faster from this area it is possible that under normal circumstances only the channels are filled with liquid. The liquid is secreted from glands that open into the channels between the blocks. Measurements have shown that the liquid viscosity $\eta \approx 0.0014$ Pa s (i.e. about 40% larger than for water) [15]. The surface tension of the liquid has not been measured but we will assume that it is similar to that of water, $\gamma \approx 0.07$ J m^{-2}.

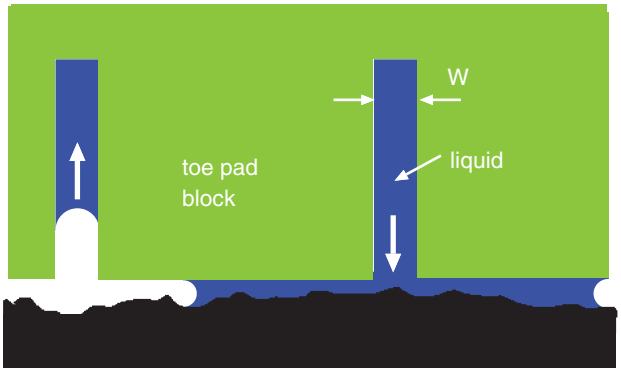

Figure 4. When the frog toe pad comes into contact with a substrate surface, liquid is pulled out from the channels because of capillary suction. If the separation h between the solid walls at the toe-pad–substrate interface is smaller than the width W of the channels, the pressure in the film between the toe pad and the substrate will be lower than in the grooves, resulting in the flow of liquid into the space between the toe pad and the substrate. Since all the grooves are connected laterally, fluid will flow laterally within the network of grooves in such a way as to conserve the volume of fluid.

2.2. Toe-pad function: qualitative discussion

The channels between the blocks (see figures 2 and 3) may have at least three functions.

(A) The bending elasticity of the toe pad on distances larger than the size of the blocks will be reduced by the channels; this will increase the toe-pad–substrate contact area and adhesion.
(B) The liquid stored in the channels will act as a liquid reservoir, which will facilitate fast adhesion to rough substrate surfaces. In section 2.3 I will discuss this point, which may be crucial for strong and *fast* adhesion to rough surfaces.
(C) The channels will facilitate the squeeze-out of fluid between the toe pad and the substrate, e.g. during raining. During fast pull-off the channels between the cells at the outer boundary of the toe pad may close, resulting in a suction-cup type of effective 'adhesion' on flooded surfaces, see section 3.

We now consider (qualitatively) the liquid flow at the interface upon forming and breaking the pad–substrate contact. When the frog toe pad comes into contact with a substrate surface, liquid is pulled out from the channels because of capillary suction, see figure 4. If the separation h between the solid walls at the toe-pad–substrate interface is smaller than the width W of the channels, the pressure in the film between the toe pad and the substrate will be lower than in the grooves, resulting in the flow of liquid into the space between the toe pad and the substrate. Since all the grooves are connected laterally, fluid will flow laterally within the network of grooves in such a way as to conserve the volume of fluid. For substrates with large enough surface roughness, there will be regions between the surfaces where the height $h(x, y) > W$, and when the fluid reaches such a region the flow will stop; see figure 5. During pull-off the liquid (or part of it) may be pulled back into the grooves by capillary forces. That is, when the separation h becomes larger than the width W of the grooves, the free energy for the system is reduced if the liquid is transferred back to the grooves; see figure 6, where the fluid flow direction is indicated by the vertical arrows. This 'conservation' of fluid may be important during fast movement, where the frog toe pads could become dry if the liquid remained trapped on the substrate surface.

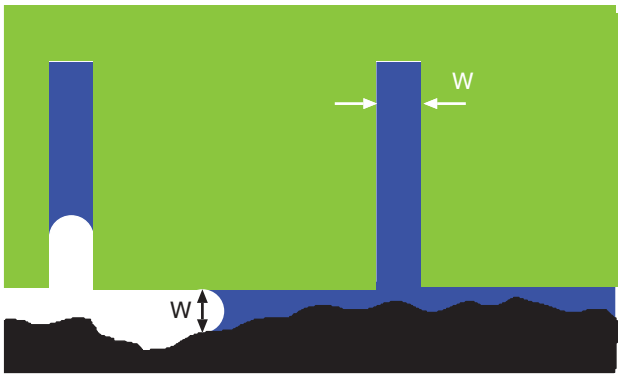

Figure 5. For substrates with large enough surface roughness, there will be regions between the surfaces where the height $h(x, y) > W$, and when the fluid reaches such a region the flow will stop.

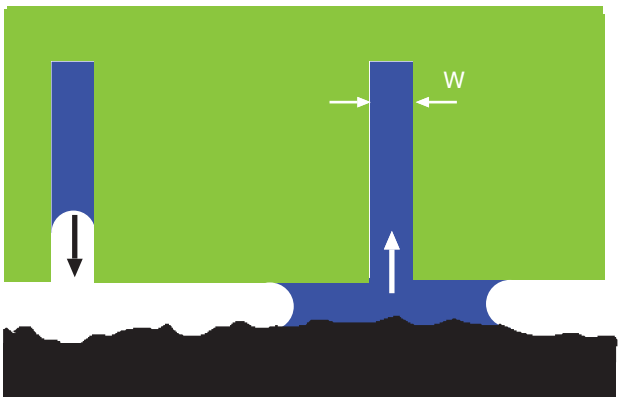

Figure 6. During separation of the toe pad from the substrate, liquid will flow back into the channels or grooves when the separation between the solid walls is larger than the width of the channels, i.e., $h > W$. The fluid flow direction is indicated by the vertical arrows.

2.3. Wet adhesion

Let us first consider the case of flat surfaces with a network of channels as illustrated in figure 7. If the width W of the channel is larger than the spacing h between the solid walls (as in figure 7), the local fluid pressure in the film between the flat surfaces will be lower than in the channel, and fluid will rapidly be sucked out from the channel. If the liquid completely wets the surfaces the pressure in the fluid in the thin interfacial film will be of order $p_1 \approx -\gamma/r$, where the radius of curvature $r = h/2$. Similarly, the pressure of the fluid in the channel will be $p_0 \approx -\gamma/r^*$, where $r^* = W/2$. The pressure difference $p_1 - p_0 < 0$ will result in fluid flow from the channel into the space between the parallel surfaces. We can estimate the flow velocity v in the thin liquid film between the solid walls using the equation

$$-\nabla p + \mu\nabla^2\mathbf{v} = \mathbf{0}$$

which in the present case, if $W \gg h$, takes the form

$$2\gamma(h^{-1} - W^{-1})/L \approx \mu 12\bar{v}/h^2 \tag{1}$$

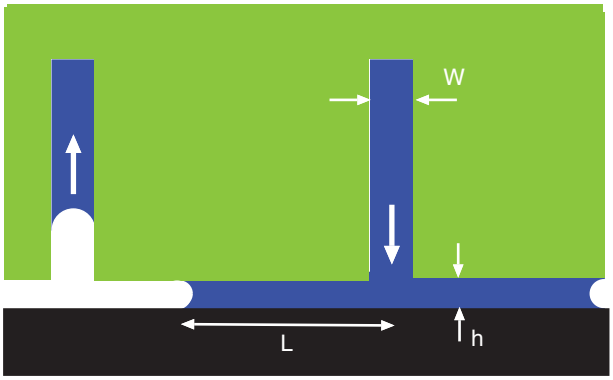

Figure 7. Model problem with fluid flow between smooth flat surfaces (see the text for details).

where $\bar{v}$ is the fluid velocity averaged over the thickness h of the film. Here we have used that the fluid velocity must vanish on the surfaces $z = 0$ and h, i.e., $v(z) = 6\bar{v}z(h - z)/h^2$. If $W \gg h$ we get from (1)

$$\bar{v} = \gamma h/6\mu L. \tag{2}$$

Next, since $v = \dot{L}$ we get from (2)

$$L\dot{L} = \gamma h/6\mu$$

or, if $L(0) = 0$,

$$L^2(t) = \gamma h t/3\mu. \tag{3}$$

Thus, the time t_0 for the liquid film to extend the distance L_0 is given by

$$t_0 = \frac{3\mu L_0^2}{\gamma h}. \tag{4}$$

We are interested in the contact between a toe pad with a network of channels, and a rough surface. If the root-mean-square roughness of the substrate surface over the lateral size of a big block (which is of order 10 μm) is denoted by h_0, then the 'natural' separation between the surfaces at the interface is likely to be of order h_0. If $h_0 \approx 0.1$ μm and if L_0 is chosen to be of order the size of the big blocks ($\sim$10 μm), we get for water ($\gamma \approx 0.07$ N m^{-1} and $\mu \approx 0.001$ Pa s) $t_0 \approx 4 \times 10^{-5}$ s. We conclude that the spreading of the liquid at the interface will occur very fast, and after a short time the liquid film will cover most of the interface. For rigid solids this will result in the maximal adhesion force of order $-p_0 A_0$, where p_0 is the (negative) pressure in the film and A_0 the nominal area of the contact region. If fluid still occurs in the large channels, $p_0 = -2\gamma/W \approx 0.1$ MPa. This stress is much larger than the stress which is obtained if the weight of a tree frog is divided by the total toe-pad area [16]: $p \approx 0.001$ MPa. Thus the capillary stress p_0 is typically $\sim$100 times larger than p. However, the bond between the toe pad and the substrate is not broken uniformly over the contact area during pull-off but rather via crack propagation (or peeling) from the periphery towards the center (see below).

Since the total force acting on the frog must vanish (as long as the frog does not move), the attractive capillary force $-p_0 A_0$ (plus the contribution from the weight of the frog) must be balanced by a repulsive force acting in the area of real (atomic) contact between the frog toe pad and the substrate. Since the regions where the solids are separated by more than just a few nanometers of (water-like) fluid will contribute with a negligible friction force during

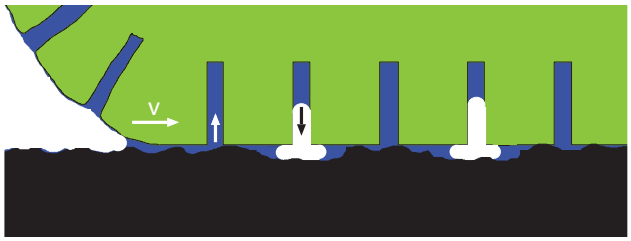

Figure 8. During pull-off an opening crack propagate (velocity v) at the pad substrate interface (see text for details).

lateral sliding, the friction force will arise almost entirely from the area of atomic contact. Experiment have shown that when a toe pad is in contact with a smooth glass surface, the area of atomic contact (where the surfaces are separated by at most $\sim$1 nm) is of order 10% of the nominal contact area [15]. For the same system, experiments have shown that the nominal frictional shear stress is of order $\sim 10^3$ Pa (which is just large enough for the tree frog to move on a vertical surface), so that the frictional shear stress in the area of atomic contact must be of order $\sim 10^4$ Pa. This shear stress is small compared to the shear stress which acts in most dry sliding contacts (where, however, the normal stresses in the contact areas are much higher (typically of order 1 GPa for glassy polymers) than in the present case), which for (glassy) polymer materials may be of order 10^7 Pa. However, the shear stress is similar to what has been observed for boundary lubricated surfaces in water. Thus, in [17] it was observed that the shear stress is of order $\sim 10^4$ Pa for mica surfaces covered by organic grafter molecules and sliding in water.

The separation of a toe pad from a substrate occurs by crack propagation (or peeling) from the periphery of the contact area. Because of stress concentration at the crack tip, this gives a much smaller pull-off force than the force $-p_0 A_0$ which would result if the bonds at the interface were to break simultaneously during pull-off. If the toe pad could be approximated as a homogeneous spherical cup, the pull-off force would be given by the JKR expression [18]

$$F = \frac{3\pi}{2} R \gamma_{\mathrm{eff}} \tag{5}$$

where γ_{eff} is the effective interfacial energy, which can be estimated as follows. Assume that the (average) separation between the solids at the interface $h \ll W$. During separation, at the crack edge the liquid film thickness is equal to W (see figure 8). Thus, the work (per unit area) necessary to separate the surfaces must be $\gamma_{\mathrm{eff}} \approx (W - h) p_0 \approx W p_0 = W 2\gamma / W = 2\gamma$. Here we have assumed that the separation speed is so low (at least until the onset of the snap-off instability) that the fluid can flow into the grooves in such a way that the film thickness always takes its equilibrium value W at the crack edge. Assuming that the radius of curvature of the toe pad is $R \approx 1$ cm and using the surface tension of water ($\gamma \approx 0.07$ N m^{-1}), we get the pull-off force for one pad $F \approx 0.006$ N. The mass of a tree frog is typically $m \sim 0.01$ kg, corresponding to the gravitational force of 0.1 N. Thus, if all the toes are attached to the substrate, the theoretical pull-off force $\sim$0.1 N may be similar to the weight of the frog.

Experiments have shown that the toe-pad material of grasshoppers is highly viscoelastic (like rubber), and the same may be true for the tree frog toe pads. Depending on the pull-off velocity, viscoelasticity of the pad material can result in a strong enhancement of γ_{eff}. For a (homogeneous) viscoelastic solid [19]

$$\gamma_{\mathrm{eff}} \approx \gamma_0 \left(1 + f(T, v)\right) \tag{6}$$

where $f(T, v)$ is due to viscoelastic deformation close to the crack tip, with $f \to 0$ as the crack tip velocity $v \to 0$. For rubber-like materials the enhancement factor f could be as large as 10^3 or 10^4. Recent experiments have shown that there may be a similar enhancement factor for the toe pad of grasshoppers and most likely for smooth adhesion pads in general. Thus, experiments by Goodwyn *et al* [14] found $\gamma_{\rm eff} \approx 10$ J m^{-2} for the toe pads of two different types of grasshoppers, and since one expects $\gamma \approx 0.07$ J m^{-2} due to capillary bridges one gets $f \approx 140$. This would result in a strongly enhanced pull-off force which would allow the tree frog to adhere to even very rough surfaces inclined at any angle relative to the earth gravitational force.

The toe-pad bulk viscoelasticity, which may result in a strong increase in $\gamma_{\rm eff}$, may also be important for sliding friction on *rough* substrates, and may result in very large sliding friction as observed for rubber materials. Thus, during sliding the substrate asperities generate pulsating deformations of the pad material, and if the pad material behave viscoelastically at the perturbing frequencies a very large friction may result, as observed for rubber sliding on rough substrates [20, 21]. We note that this is the case even if the pad and the substrate are separated by a very thin viscous liquid film, assuming that the film thickness is smaller than the size of the (relevant) substrate asperities. This effect has, in fact, been observed in a recent experiment for rubber lubricated by different organic oils and sliding on a rough substrate.

3. Contact mechanics and adhesion on flooded substrates

Tree frogs can adhere and move on rough (hard) vertical surfaces during heavy raining where the surfaces are flooded with water. This cannot be explained by the capillary-bridge picture since no capillary bridges can form on a flooded surface. Here we will discuss how the adhesion may be generated for flooded surfaces. We first consider the liquid squeeze-out, which is a prerequisite for non-negligible adhesion and friction.

We consider the squeeze-out of a liquid from the interface between a solid with a flat surface, and another solid with a surface with a network of (draining) channels. We assume first that the inertia of the fluid can be neglected but we include the fluid viscosity. We also consider the opposite case where the viscosity can be neglected but we include the inertia of the fluid in the analysis.

3.1. Viscosity-dominated squeeze-out

Consider the squeeze-out of liquid from the space between two solid bodies. Assume first rigid solids with perfectly flat surfaces without draining channels. Since in the present applications the pressure is low, we can assume an incompressible liquid so that

$$\nabla \cdot \mathbf{v} \approx 0 \tag{7}$$

$$-\nabla p + \mu \nabla^2 \mathbf{v} \approx \mathbf{0}. \tag{8}$$

Assume that $h(t)$ is the separation between the surfaces at time t. We will use simple (dimensional) arguments to obtain an approximate form of $h(t)$. Assume that the nominal contact region is circular with the diameter D_0. Assume that $h(t)$ changes by the amount $\Delta h < 0$ during the time interval Δt. Fluid mass conservation gives

$$-D_0^2 \Delta h \approx D_0 h v \Delta t$$

or

$$\dot{h} \approx -hv/D_0, \tag{9}$$

where v stands for the radial component of the fluid velocity averaged over the thickness $0 < z < h$ of the fluid film. Since the flow velocity vanishes on the surfaces $z = 0$ and h, the strongest spatial variation in $\mathbf{v}(\mathbf{x}, t)$ will be derived from the variation of $\mathbf{v}$ with z so that, from dimensional arguments, $\nabla^2\mathbf{v} \sim v/h^2$. Thus, (8) gives $p/D_0 \approx \mu v/h^2$, where $p = F_N/\pi D_0^2$ is the squeezing pressure. Combining this with (9) gives

$$\dot{h} \approx -\frac{\alpha p}{\mu D_0^2} h^3 \tag{10}$$

where α is a number of order unity. An accurate calculation gives $\alpha = 4/3\pi$. If the external load F_N is constant it is easy to integrate (10) to get

$$\frac{1}{h^2(t)} - \frac{1}{h^2(0)} \approx \frac{\alpha p t}{\mu D_0^2}. \tag{11}$$

Next let us assume that the substrate surface has vertical draining channels as in figure 7. Let us first consider the situation where h is so small (but not too small—see below) that nearly all the squeeze-out of the fluid occur via the channels. Consider first the flow in one channel. We assume that the height H_1 of the channel is much larger than its width W_1; see figure 7. In this case we expect the strongest spatial variation of $\mathbf{v}(\mathbf{x}, t)$ to be derived from the variation of $\mathbf{v}$ with y so that, from dimensional arguments, $\nabla^2\mathbf{v} \sim v/W_1^2$, where v is the flow velocity in the channel, averaged over the channel cross section area $H_1 W_1$. Thus, (8) takes the form

$$p/D_0 \approx \mu v/W_1^2. \tag{12}$$

Let us now assume a network of channels on the surface forming a square (or hexagonal) lattice with the 'lattice constant' D_1. Fluid mass conservation gives $-\dot{h} D_0^2 \approx N v H_1 W_1$, where $N \approx D_0/D_1$ is the number of channels crossing the outer boundary of the nominal contact area. Thus we get

$$\dot{h} \approx -v\frac{H_1 W_1}{D_0 D_1}. \tag{13}$$

From (12) and (13) we get

$$\dot{h} \approx -\frac{p W_1^3 H_1}{\mu D_0^2 D_1} = -\frac{\alpha p}{\mu D_0^2} h_0^3 \tag{14}$$

where we have defined

$$h_0 = \left(\beta \frac{W_1^3 H_1}{D_1}\right)^{1/3} \tag{15}$$

where the dimensionless number β is of order unity. We can interpolate smoothly between the limits (10) and (14) by using

$$\dot{h} \approx -\frac{\alpha p}{\mu D_0^2} (h + h_0)^3 . \tag{16}$$

Thus, the draining channels will effectively increase the separation between the surfaces by distance h_0, and hence facilitate the squeeze-out. Equation (16) is only valid until the film thickness h reaches some lower critical value h_1, which can be determined as follows. For $h > h_1$ (but $h < h_0$) the 'bottleneck' for squeeze-out is the viscous resistance to fluid flow in the channels. For $h < h_1$ the 'bottleneck' for squeeze-out is instead the viscous squeeze-out (transfer) of the liquid from the block–substrate $D_1 \times D_1$ interface area to the channels. To study this quantitatively, let us consider the squeeze-out of the liquid film from a basic unit (area $\sim D_1^2$) to the surrounding draining channels. If the film is very thin the squeeze-out is very slow and the fluid pressure in the draining channels will be similar to the external (atmospheric)

pressure. In this case the squeeze-out of the thin fluid film into the draining channels will be mathematically identical to the squeeze-out of the liquid between smooth surfaces studied above (equation (10)), but with D_0 replaced by D_1. Thus, for a very thin fluid film we have

$$\dot{h} \approx -\frac{\alpha p}{\mu D_1^2} h^3. \tag{17}$$

We can determine h_1 by the condition that the squeeze rates (14) and (17) are equal:

$$h_1^3/D_1^2 \approx h_0^3/D_0^2$$

or

$$h_1 = h_0 \left(\frac{D_1}{D_0}\right)^{2/3} = \left(\frac{\beta W_1^3 H_1 D_1}{D_0^2}\right)^{1/3}. \tag{18}$$

From the analysis above it is clear that if the squeeze-pressure p (or the force F_N) is constant the fluid film thickness will first decrease with time as $\sim t^{-1/2}$ until $h(t)$ reaches $\sim h_0$, which takes the time

$$t_0 \approx \frac{\mu D_0^2}{\alpha p h_0^2}. \tag{19}$$

From here on the squeeze-out will occur mainly via the draining channels, and $h(t)$ will decrease linearly with time until $h(t) \approx h_1$. If $h_1 \ll h_0$ the time t_1 it takes to decrease $h(t)$ from h_0 to h_1 will be (from (14)) of order $t_1 \approx t_0$, so the total squeeze-out time to reach $h = h_1$ will be of order $2t_0$. If the basic $D_1 \times D_1$ units have perfectly flat surfaces, for $t > 2t_0$ the squeeze-out will again follow the $t^{-1/2}$ time dependence. However, the squeeze-out will occur faster if the $D_1 \times D_1$ surface units have draining channels with appropriate width W_2, depth H_2 and density (see below). It is clear that for maximum squeeze-out speed the system should have a hierarchical distribution of draining channels where a basic unit surrounded by 'large' draining channels has a network of much smaller draining channels and so on. The theory above can be used to estimate the squeeze-out time for such complex hierarchical systems. We also note that to some extent the channels can be replaced by surface roughness. However, in this case the squeeze-out channels will not have a uniform size but will exhibit strong fluctuations, leading to the possibility of trapped liquid (liquid islands), in particular when the elastic deformation of the solids is taken into account. Such trapped or 'sealed off' water islands have recently been suggested to be the origin of why tires on wet roads at low car velocities exhibit ~20–30% smaller friction than for dry road surfaces (the trapped water effectively smooths the road surface profile, resulting in less asperity-induced viscoelastic deformation of the rubber).

As an application, consider the tree frog toe pad. In this case $D_0 \approx 1$ mm, $D_1 \approx 10\ \mu$m, $H_1 \approx 5\ \mu$m and $W_1 \approx 1\ \mu$m. Thus, $h_0 \approx 1\ \mu$m and $h_1 \approx 50$ nm. Using the measured viscosity (similar to that of water) $\mu = 0.0014$ Pa s, and $p = 10^4$ Pa (typical frog toe squeezing stress), we get the squeeze-out time $2t_0 \approx 0.1$ s.

Assume that the film thickness $h < h_1$. In this case, for $D_1 \times D_1$ units with perfectly flat surfaces the bottleneck in the squeeze-out is the transfer of the liquid to the draining channels. In this case the squeeze-out will speed up if, in addition to the large draining channels discussed earlier, the substrate is covered by a network of smaller channels (width W_2 and depth H_2) with 'lattice constant' D_2. For this case, for the time interval where $h_1 < h < h_2$ (where h_2 is defined below), the film thickness satisfies

$$\dot{h} \approx -\frac{\alpha\beta W_2^3 H_2 p}{\mu D_1^2 D_2}. \tag{20}$$

This equation only holds as long as $h > h_2$, where h_2 is determined in an analogous manner to how h_1 was determined. Thus, when $h = h_2$ the rate (20) equals the squeeze rate for a flat surface of size $D_2 \times D_2$:

$$\dot{h} \approx -\alpha \frac{ph^3}{\mu D_2^2}.$$

This gives

$$h_2 \approx \left(\frac{\beta W_2^3 H_2 D_2}{D_1^2} \right)^{1/3} \tag{21}$$

and the time to reduce the film thickness from h_1 to h_2 will be of order

$$t_2 \approx \frac{\mu D_1^2 D_2 h_1}{\alpha \beta H_2 W_2^3 p}. \tag{22}$$

For the frog toe pad, $H_2 \approx D_2 \approx 200$ nm and $W_2 \approx 50$ nm. Using $p \approx 10^4$ Pa and $\mu \approx 0.0014$ Pa s, we get $h_2 \approx 6$ nm and $t_2 \approx 0.001$ s. Thus, we conclude that within $\sim$0.1 s the tree frog is able to squeeze out the liquid from the toe-pad contact area down to a distance of order a few nanometers. This analysis has neglected both surface roughness and the finite elasticity of the solid walls. It is well known that for elastically soft solids the latter may be very important, and studies for rubber have shown that it can give rise to (dynamically) trapped liquid islands in the contact region.

3.2. Inertia-dominated squeeze-out

In the study presented in section 3.1, all the resistance to squeeze-out comes from viscous dissipation as the fluid flow between closely spaced surfaces. Assuming no slip, the fluid velocity must vanish on the solid surfaces, which will result in very large shear velocity gradients in the narrowest spacings, and this leads to large viscous energy dissipation and to large resistance against squeeze-out. For squeeze-out at large separation between the solid walls, and for high squeeze-out velocities, it is instead the inertia of the liquid which will determine the squeeze-out speed. Thus, to remove the liquid rapidly between solid surfaces, very large acceleration of the liquid is necessary. This limiting case is not relevant for tree frog adhesion (see below), but may be very important for the squeeze-out of the water between tires and flooded road surfaces. This problem can also be studied using simple (dimensional) arguments.

Consider first a fluid layer (thickness $h(t)$) between perfectly flat solid walls squeezed together with the force F_N. The variation of $h(t)$ with time can be obtained (approximately) from the following very simple energy conservation condition. The work to squeeze the solids together by the distance $-\Delta h$ is given by $-F_N \Delta h$. We assume that this energy is converted into translational energy of the (squeeze-out) liquid. If v is the radial velocity of the liquid at the edge $r = R_0 = D_0/2$ of the contact zone then the kinetic energy of the liquid leaving the contact zone during the time period Δt becomes $\Delta m v^2/2$, where $\Delta m = \rho 2\pi R_0 h v \Delta t$ is the mass of the squeezed-out liquid. Energy conservation gives

$$-F_N \Delta h \approx \Delta m v^2/2$$

or

$$\frac{\dot{h}}{h} = -\frac{v^3 \rho}{R_0 p} \tag{23}$$

where the squeezing pressure $p = F_N/\pi R_0^2$. Mass conservation gives $\pi R_0^2(-\Delta h) = 2\pi R_0 h v \Delta t$ or

$$v = -\frac{R_0}{2}\frac{\dot{h}}{h}. \tag{24}$$

Combining (23) and (24) gives

$$\dot{h} = -h/\tau \tag{25}$$

where the characteristic squeeze-out time

$$\tau = \left(\frac{R_0^2\rho}{8p}\right)^{1/2}. \tag{26}$$

From (25) we get

$$h(t) = h(0)\mathrm{e}^{-t/\tau}. \tag{27}$$

Rubber friction on wet road surfaces is due to the viscoelastic deformation of the rubber by the road surface asperities. Since road surfaces are fractal-like, a wide distribution of asperity sizes occur but a detailed study has shown that typically only surface roughness wavelength components larger than $\sim$1 μm will contribute to the rubber friction. The analysis below shows that when the water film thickness reaches $\sim$10 μm the squeeze-out dynamics is dominated by the water viscosity rather than the water inertia. Thus, if the initial water film on the road has the thickness $\sim$1 cm it will take time $t \approx \tau \ln(10^4) \approx 7\tau$ to squeeze out the water down to the film thickness of order 10 μm. If we assume $R_0 \approx 0.1$ m and $p \approx 0.4$ MPa, this gives squeeze-out time $\sim$0.01 s. During rolling at speed v the squeeze-out time for slick tires (i.e. tires without tread pattern) is of order $2R_0/v$. Thus, for slick tires the car velocity can be at most 20 m s^{-1} or $\sim$60 km h^{-1} in order for the water film thickness to become of order (or smaller than) 10 μm. This rough estimate is in good agreement with experimental observations, but a more complete treatment should include the substrate roughness in the analysis, which will tend to speed up the squeeze-out.

Note that the condition $7\tau \approx 2R_0/v$ can be written as

$$v \approx (p/\rho)^{1/2} \tag{28}$$

which does not depend on the size R_0 of the tire–road footprint.

Tires for passenger cars have draining channels to speed up the removal of water from the tire–road footprint area under wet road conditions; see figure 9. In this context the word 'draining' is actually not appropriate as the function of the channels is not to drain the water from the footprint area but to move the water from one region in the footprint area to another region in the footprint where it can cause no harm. That is, the channels or voids act as empty volumes into which the water under the tread blocks in the footprint area can be transferred without accelerating it to such high speed as would be necessary for slick tires (i.e. tires without tread pattern). If the water film thickness on the road surface is small enough, the water under the tread blocks can be transferred to the channels without completely filling them. In this case the squeeze-out formula derived above can still be used, but with R_0 being replaced by the lateral size of a tread block, which typically is of order $a \sim 2$ cm. Thus the squeeze-out speed is increased by a factor of $R_0/a \sim 5$ and a complete separation of the tire from the road (aquaplaning) will not occur under normal driving circumstances, unless the water film is so thick that there is not enough space for it in the channels. We note that while the size of the tread block matters a lot for the ability to remove the water, the actual tread design is not very important and is decided by the tire makers' marketing people. Winter tires have in addition to the large wide channels typical of summer tires a dense network of very thin vertical cuts. It

Figure 9. Tire with a network of wide and narrow channels.

is clear that these cuts cannot absorb any large volume of displaced water (as compared to the large more widely spaced channels), but may be very important to increase the tire–road grip on snow-covered road surfaces.

Equation (25) is valid when the film thickness is so large that the liquid viscosity can be neglected. Equation (10) is valid in the opposite limit, where the film thickness is so small that the squeeze-out is dominated by the fluid viscosity. The (critical) film thickness h^* where one switches from inertia-dominated squeeze-out ($h > h^*$) to viscosity dominated squeeze-out ($h < h^*$) is obtained when the two squeeze-out speeds (10) and (25) become equal. We get

$$h^* \approx \left(\frac{(\mu R_0)^2}{p\rho}\right)^{1/4}. \tag{29}$$

For tire applications this gives $h^* \approx 10\ \mu$m. Thus, if the initial water film thickness is 1 mm the theory developed in section 2.1 cannot be used to determine the film thickness until we reach the viscosity-dominated era, which starts when $h \approx 10\ \mu$m; see figure 10. For the frog adhesive pad with $R_0 \approx 1$ mm and $p \approx 10^4$ Pa we get $h^* \approx 10\ \mu$m. However, the theory above shows that the reduction in the film thickness from 1 mm to 10 μm takes less than 0.001 s, so the inertia-dominated squeeze-out era can be neglected.

3.3. Adhesion on flooded surfaces

It has been observed that tree frogs are also able to adhere and move on vertical solid walls during heavy rain, where the substrate surface is flooded by water [16]. The reason for this is non-trivial, because under flooded conditions it appears (but see below) that no capillary bridges can form and one would therefore expect a negligible force to separate the surfaces, at least during slow separation. Here I will analyze this remarkable problem and suggest some explanations.

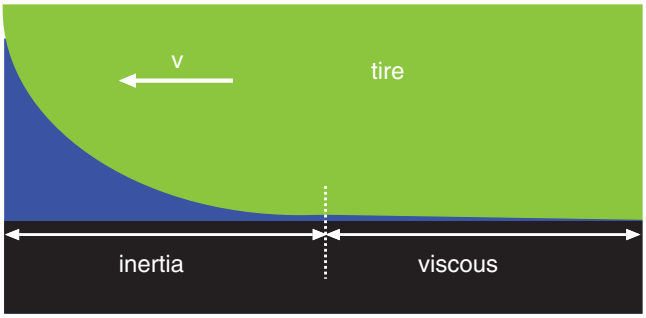

Figure 10. When a tire is rolling or sliding on a wet substrate, the liquid will be squeezed out from the (apparent) contact region between the tire and the road. In general one can distinguish between two regions: a region close to the front of the tire–road footprint area, where the squeeze-out dynamics is dominated by the inertia of the water, and another region, where the water film thickness is very small and where the viscosity of the water determines the squeeze-out dynamics.

3.3.1. Long-range interactions between solids in liquids. Solid surfaces in water sometimes interact with long-range forces derived from ion absorption on their surfaces [22]. Such forces can be both attractive (if the charges of the adsorbed ions on the two surfaces have opposite sign) and repulsive [22]. However, it is very unlikely that such forces are of any relevance for attachment systems in animals because animals must be able to adhere to many different types of surface (such as stone or leaf) with very different properties, and it is highly unlikely that these surfaces, if at all charged, would have the same sign of the charges (and opposite to that of the animal toe-pad surface).

The long-range van der Waals interaction will also act between solids separated by a thin water layer. While the van der Waals interaction *always* is attractive between solids in vacuum, it can be either attractive or repulsive in a liquid [23]. However, it is highly unlikely that this interaction is important for animals which secrete a liquid because if it would be important in water, it would (usually) be even more important when no liquid separate the surfaces, and the animal would not need to secrete any liquid at all. Thus, it is highly unlikely that any long-range interaction is of important for animal locomotion on water covered surfaces.

3.3.2. Dewetting transition. Complete liquid removal from the region between closely spaced solids has been studied both experimentally and theoretically for several years [24, 25]. A liquid film confined between two elastic solids with flat surfaces is thermodynamically unstable if

$$\gamma_{1L} + \gamma_{2L} - \gamma_{12} > 0, \tag{30}$$

where γ_{1L} and γ_{2L} are the solid–liquid interfacial energies and γ_{12} the solid–solid interfacial energy. In this case squeeze-out of the liquid may start by the formation (due to a thermal fluctuation) of a small dry patch, which then spreads laterally until the whole liquid film is expelled. However, for water this relation is unlikely to be obeyed for all surfaces to which the animal must be able to adhere. Thus stones, for example, are likely to have polar surfaces which are wet by water, and it is unlikely that (30) will be obeyed for these substrates. In addition, if the liquid were removed by a dewetting transition, then the contact region would be dry, but we already know that the adhesion for the dry contact most likely is negligible (it is for this reason that the tree frog injects a wetting liquid into the contact area).

3.3.3. Viscous 'adhesion'. When two closely spaced surfaces are separated rapidly in a liquid, strong effective adhesion may occur between the solids. The origin of this effect is the viscosity

of the liquid: because of the viscosity, if the separation between the surfaces is very small it will take a long time for the liquid to flow into the 'empty space' generated during the separation between the solids. This can result in a large negative pressure and even cavity formation between the surfaces of the solids [26, 27]. This 'viscous adhesion' is a dynamical effect and disappears if the surfaces are separated very slowly. For rigid flat walls the magnitude of the attraction can be estimated from (10): when $\dot{h} > 0$ (separation) (10) gives $p < 0$, i.e. an effective attraction prevails between the solid surfaces during separation. A large pull-off force is only observed if the separation h between the solid is very small (or the pull-off speed very high). That is, before strong adhesion is possible the liquid must be nearly completely removed (squeezed out) from the region between the surfaces. An accurate analysis of this problem requires in general that one includes the elastic deformation of the solids when determining the pull-off force.

In section 3.1 we showed that the squeeze-out is facilitated by a network of draining channels on the surface of the adhesion pad. Here we note that while these channels are 'open' during squeeze-out they may be closed during pull-off, at least close to the boundary of the contact region. The reason for this is that during pull-off there is lower pressure inside the contact area than outside, and there will be lateral (radial) forces acting tending to compress the contact area laterally, and this may close the space between the hexagonal units. This will slow down the flow of liquid into the region between the surfaces, which may strongly increase the pull-off force.

4. Summary and conclusion

Tree frogs and most insects use wet adhesion to adhere and move on many different surfaces, e.g. glass windows, stone walls or plant leaves. I have discussed the origin of adhesion and friction for the tree frog but the results may be relevant for other animals using smooth adhesion pads, e.g. grasshoppers. In fact, the similarity between the adhesion pads of tree frogs and grasshoppers is very great, indicating highly optimized (by natural selection) and unique adhesive systems. Some of the results presented above may also be relevant for some technological applications, e.g. tires on wet road surfaces.

Acknowledgments

I thank W Federle and S Gorb for useful communications.

References

[1] Persson B N J 2002 *Eur. Phys. J.* E **8** 385
[2] Persson B N J 2006 *Surf. Sci. Rep.* **61** 201
[3] Fuller K N G and Tabor D 1975 *Proc. R. Soc.* A **345** 327
[4] Gorb S 2001 *Attachment Devices of Insect Curtile* (Dordrecht: Kluwer)
Scherge M and Gorb S 2001 *Biological Micro- and Nano-Tribology* (Berlin: Springer)
[5] Persson B N J 2003 *J. Chem. Phys.* **118** 7614
[6] Persson B N J and Gorb S 2004 *J. Chem. Phys.* **119** 11437
[7] Carbone C and Persson B N J 2004 *Phys. Rev.* B **70** 125407
[8] Autumn K, Sitti M, Liang Y A, Peattie A M, Hansen W R, Sponberg S, Kenny T W, Fearing R, Israelachvili J N and Full R J 2002 *Proc. Natl Acad. Sci.* **99** 12252
[9] Gorb S N 1998 *Proc. R. Soc.* B **265** 747
[10] Federle W 2006 *J. Exp. Biol.* **209** 2611
[11] Persson B N J 2007 *MRS Bull.* **32** 486

[12] Vötsch W, Nicholson G, Müller R, Stierhof Y-D, Gorb S and Schwarz U 2002 *Insect Biochem. Mol. Biol.* **32** 1605
[13] Federle W, Riehle M, Curtis A S G and Full R J 2002 *Integr. Comp. Biol.* **42** 1100
[14] Goodwyn P P, Peressadko A, Schwarz H, Kastner V and Gorb S 2006 *J. Comp. Physiol.* A **192** 1233
[15] Federle W, Barnes W J P, Baumgartner W, Drechsler P and Smith J M 2006 *J. R. Soc. Interface* **3** 689
[16] Barnes J 1999 *Tire Technology International* pp 42–7
[17] Briscoe W H, Titmuss S, Tiberg F, Thomas R K, McGillivray D J and Klein J 2006 *Nature* **444** 191
[18] Johnson K L, Kendall K and Roberts A D 1971 *Proc. R. Soc.* A **325** 301
Johnson K L 1985 *Contact Mechanics* (Cambridge: Cambridge University Press)
[19] See, e.g. Persson B N J, Albohr O, Heinrich G and Ueba H 2005 *J. Phys.: Condens. Matter* **17** R1071
Persson B N J and Brener E 2005 *Phys. Rev.* E **71** 036123
[20] Persson B N J 2001 *J. Chem. Phys.* **115** 3840
[21] Persson B N J, Albohr O, Tartaglino U, Volokitin A I and Tosatti E 2005 *J. Phys.: Condens. Matter* **17** R1
[22] See, e.g. Persson B N J and Mugele F 2004 *J. Phys.: Condens. Matter* **16** R295
[23] Israelachvili J 1992 *Intermolecular and Surface Forces* (London: Academic)
[24] Brochard-Wyart F and de Gennes P G 1994 *J. Phys.: Condens. Matter* **6** A9
Martin P and Brochard-Wyart F 1998 *Phys. Rev. Lett.* **80** 3296
Martin P, Buguin A and Brochard-Wyart F 2001 *Langmuir* **17** 6553
[25] Persson B N J, Volokitin A and Tosatti E 2003 *Eur. Phys. J.* E **11** 409
Carbone C and Persson B N J 2004 *J. Chem. Phys.* **121** 2246
[26] Persson B N J 2000 *Sliding Friction: Physical Principles and Applications* 2nd edn (Heidelberg: Springer)
[27] Smith A M 1991 *J. Exp. Biol.* **157** 257
Caupin F and Herbert E 2006 *C. R. Phys.* **7** 1000